Influence of the Ringer's solution on wear of vacuum mixed poly(methyl methacrylate) bone cement in reciprocating sliding contact with AISI 316L stainless steel

Fatima Zivic[1], Nenad Grujovic[1], Slobodan Mitrovic[1], Jovan Tanaskovic[2] and Petar Todorovic[1]

[1]*University of Kragujevac, Faculty of Engineering, Kragujevac, Serbia*
[2]*University of Belgrade, Faculty of Mechanical Engineering, Belgrade, Serbia*

Abstract

This paper presents microstructural properties and damage behaviour of a vacuum mixed poly(methyl metacrylate) (PMMA) bone cement, during the sliding contact with AISI 316L stainless steel, under micro-loads. Influence of the Ringer's solution on the wear was analysed in comparison to dry contact. The variation of load did not produce any significant change of the wear factor while the increase in the sliding speed induced significant increases in the wear factor, more pronounced in the case of dry sliding. The obtained wear factors were in average higher for the sliding in Ringer's solution than those obtained under dry conditions. Significant fragmentation of the worn tracks, of irregular shapes with broken edges, was observed, slightly more pronounced for the dry contact. Many cavities and voids were formed on the wear track surface, but they did not extend into the bulk material. Higher loads produced more uniform and less fragmented wear tracks. Abrasive, adhesive wear and plastic deformation grooves were observed, as well as fatigue and erosive wear. Fatigue cracks developed in the direction normal to sliding. Network of fine craze cracks was exhibited on the surface of wear tracks, especially pronounced in the case of dry sliding. These results are important since they contribute to understanding the sites of crack initiation, and development mechanisms on the surface of PMMA bone cements, also including synergistic effects of physiological environments pertaining to the non-steady crack and craze behaviour and crack pattern development in PMMA.

Keywords: craze cracks; erosive grooves; fracture; densification; friction heating; fatigue crack.

Available on-line at the Journal web address: http://www.ache.org.rs/HI/

ORIGINAL SCIENTIFIC PAPER

UDC: 678.744.32+ 691.714.018.8: 620.178.16

Hem. Ind. **75 (2)** 77-92 (2021)

1. INTRODUCTION

Polymers for biomedical applications are designed to be either biostable or bioabsorbable. Biologically stable polymers provide a permanent support during the life-time of the patient. Poly(methyl methacrylate) (PMMA) $[(C_5O_2H_8)_n]$ based bone cements belong to a group of synthetic nondegradable, biocompatible polymeric hard biomaterials. Acrylic bone cements have versatile applications such as: cemented hip implants [1], spinal treatments [2], custom made bone implants [3], dental applications like orthodontic brackets [4] and occlusal splints [5]. PMMA is an isotropic, elasto-visco-plastic solid and amorphous/glassy polymer material. Bone cement is basically a mixture of PMMA powder obtained by in situ polymerization of the monomer methyl methacrylate (MMA). Diameter of PMMA beads usually lies in the range of 1 - 125 μm. These beads are soluble in the MMA monomer. The resulting polymer is amorphous, optically transparent, has a high refraction index, is hard and brittle and suitable for a number of biomedical applications. The bone cement commercially used is a complex mixture of the monomer, PMMA powder, an initiator, a promoter of polymerization (or curing), a protector to prevent premature polymerization during mixing and a filler [2]. They are mixed prior to use under well controlled conditions mainly to prevent the formation of large pores and voids,

Corresponding author: Fatima Zivic, University of Kragujevac, Faculty of Engineering, Sestre Janjić 6, 34000 Kragujevac, Serbia
E-mail: zivic@kg.ac.rs
Paper received: 05 January 2021
Paper accepted: 24 March 2021
https://doi.org/10.2298/HEMIND210105011Z

since these would significantly affect mechanical properties of the final product. An effective technique to decrease the bone cement porosity is vacuum mixing during the material preparation [6] and different benefits of such a procedure have been reported [1,2].

According to many literature resources, appearance of cement defects is highly related to the implant loosening and osteolysis [7,8]. Osteolysis is a process of bone matrix destruction, or removal of the bone mineralized matrix and destruction of the organic bone phase (composed of ~90 % collagen). Predicting the long-term mechanical behaviour of an implant is difficult because reported studies indicate large variations in mechanical properties of the interface between the bone matrix and the implant [7]. In the case of cemented joint prosthesis, essential properties which determine *in vivo* stability are related to the bone cement fatigue and fracture behaviour and many investigations are focused on the cause of failure and micromechanics [9]. Porosity and various material defects (*e.g*. agglomerates of radiopaque phases) have a prominent role in the process of crack development. It has been shown experimentally that cements with lower porosities exhibit better compressive and flexural properties [9,10]. However, relations of the porosity reduction to void size, morphology, number or spatial distribution are rarely specified, usually considering only one of these variables. Addition of radiopaque agents and different additives to PMMA bone cements further increases the complexity of material responses [2].

The role of the bone cement is to transfer complex load forms between the prosthesis and the bone. The loosening process is still under consideration, even though specific aspects have been determined, such as fracture and fatigue behaviour of PMMA cements [10]. Nguyen et al. [10] considered a cyclic fatigue crack growth as the major governing factor of the bone cement failure, considering approximately five million steps per year for one person, meaning that the joint prosthesis should endure around 10^8 cyclic motions during its lifetime. Also, in dentistry, steel brackets are in close contact with PMMA [4]. On the other hand, articulating surfaces of loose joint replacements generate wear debris during the contact. The particulate wear debris produced during the micro-contact between the loose cement surfaces and bone can have different unwanted effects. Part of that particulate wear debris consists of the bone cement particles, originating from the low amplitude reciprocating motion under low loads of the loose implant. The extent and rate to which cement particles are generated determine the life of the prosthesis.

In other cases of custom implants made of PMMA bone cements, such as thoracic bones, the implants are connected to the remaining bones usually by using metal wires (*e.g*. sternal wires made of AISI 316L stainless steel) [3]. The connection is made by drilling holes through the cement implant on one side and the living bone on the other, where the sternal wires are tightly setup, but certain wire micro-motions over the cement must exist during normal daily activities. Therefore, in such cases, the tribological behaviour of the contact pair PMMA bone cement - AISI 316L stainless steel determines the life of sternal wires which hold the implant at place. The potential fracture mechanism of such sternal wires was reported to be based on the presence of crevice corrosion and severe transversal cracks detected in broken wires [11].

Friction and wear mechanisms are largely unexplored in the case of PMMA bone cements, even though there are several studies related to specific aspects, such as corrosion influence on the friction behaviour or the effects of oscillatory motion at small amplitude, during the contact between AISI 316L steel and PMMA [12]. There are several studies on the friction coefficient dependence on hardness, surface roughness and chemical reaction of AISI 316L steel for bone screws [13] as well as on wear of occlusal splints and PMMA in dentistry [5,14]. Still, formation of a third body between articulating surfaces as well as different superposing influences such as that of a corrosive environment have to be included in considerations. The presence of a third body usually enhances further particle production as reported in studies of the accompanying phenomena and ways to reduce wear [8]. Phenomena such as wear and fracture mechanisms of PMMA bone cements need to be fully understood to quantify the occurring wear debris.

Questions related to sites of crack initiation, development mechanisms and the final failure point in the case of PMMA bone cements still remain, even though there are many studies focused on some specific aspects, like the surface finish in dental applications [4], or mechanisms that govern crack branching [15]. Some reports indicate that the start of separation of the cement from the metal stem is initiated by large fractures within the cement layer [10]. In the case of the cemented metal prosthesis, there are several opinions on the initiation site of the cement crack: (1) on the surface

of the loose cement; (2) in voids associated with porosity in the cement layer or at the metal-cement interface; or (3) in the vicinity of a pore in the cement [9, 10]. Yet another issue is related to the presence of stress concentrations within the bone cement that is related to porosity, different additives, and radiopaque agents. Nonsteady crack and craze behaviour in PMMA, crack growth rate and crack pattern development, additionally including synergistic effects of physiological environments have not been well understood yet [16] and better understanding of these phenomena are needed. From the materials engineering point of view, it is of great interest to relate the material performance to the microstructure, helping to understand all parameters that influence the long-term sustaining of loads and to prolong the implant durability.

This paper presents the influence of Ringer's solution on contact phenomena between a vacuum treated PMMA bone cement and AISI 316L stainless steel during reciprocating sliding. A micro-scale load range was applied, under dry and wet contact. Wear mechanisms were investigated in response to different normal force and linear speed values applied.

2. EXPERIMENTAL

2. 1. Materials

Commercially available PMMA bone cement for orthopaedic surgery (Palacos R, Schering Corporation, USA) was used as a test material. The PMMA bone cement is composed of: polymer powder components (methylacrylate - copolymer (PMMA beads); benzoyl peroxyde; zirconium dioxyde and chlorophyll) and liquid components (methyl methacrylate monomer; N,N-dymethyl-p-toludine and chlorophyll). The mixing procedure was performed according to the instructions of the manufacturer and by applying vacuum. Details of the material preparation procedure are reported previously [6]. The vacuum treated cement used in this study had the final porosity of 5.1 % and surface roughness of Ra = 10.5 μm. Flat block samples (30 mm x 20 mm x 15 mm) were prepared for testing in accordance with ASTM F732-00, ASTM F86-01 and ASTM F2025-00 standards. Each PMMA sample was washed with neutral soap and water. They were stored in a desiccator, prior to testing.

2. 2. Reciprocating sliding contact

Sliding tests of the flat cement samples were realised by using the ball-on-flat configuration at CSM Nanotribometer (CSM, Switzerland). Details of the device configuration are presented previously [17]. Tribological tests realised linear reciprocating sliding of the ball (AISI 316L stainless steel ball; diameter of 1.5 mm) on the flat PMMA sample, with dry contact and in Ringer's solution (simulation of body fluid environment; purchased, Hemofarm AD Vrsac, Serbia), at room temperature (approximately 25 °C). We tested five values of the normal load, Fn (100, 250, 500, 750, and 1000 mN) and three values of the maximal linear speed, v (4, 8 and 12 mm/s). Calculated values of the maximum elastic contact stress (according to the applied normal loads) were: 71.9, 97.6, 123.0, 140.8, and 154.9 MPa, respectively. Duration of each test was 10000 cycles (total distance of 16 m), where the one cycle is represented by two full amplitudes of the sliding distance (*i.e.* half amplitude, 0.4 mm; full amplitude, 0.8 mm; 1 cycle, 1.6 mm). Sliding speeds were selected as the most probable motion range within a body. Laboratory investigations using Ringer's solution instead of fat-based solutions represent the worst-case scenario [18]. The composition of the Ringer's solution used is as follows: 8.6 g dm^{-3} NaCl, 0.30 g dm^{-3} KCl and 0.33 g dm^{-3} $CaCl_2$. Articulating surfaces were completely immersed in the solution during sliding. A ball-on-flat contact configuration at a nanotribometer is commonly used to represent the circular contact point between a rigid sphere (alumina ball) and a flat sample (PMMA) and is modeled by the Hertzian contact theory in contact mechanics. Therefore, the contact zone was immersed in the solution, by applying 5 cm^3 of Ringer's solution on the flat sample at the beginning of each test, since it was shown by our previous tests that this quantity of the solution can provide full immersion of the contact pair during the whole test. Tests were repeated three times.

Optical images of the wear track on a PMMA sample were recorded after each test by using optical microscope (Meiji Techno MT-8530). It is important to note that care is required during the scanning electron microscopy (SEM) examination of the surface, since an intense electron beam will cause PMMA sample to decompose. The samples for

the SEM analysis were prepared, by coating them with an ultra-thin layer of gold, by a sputter coater LEICA EM SCD005 (Leica Microsystems, Austria), immediately prior to the SEM imaging at Scanning Electron Microscope JSM-6610LV, with EDS, JEOL Ltd, Japan. EDS analysis was also performed. Nanotribometer continuously measures the penetration depth (PD) parameter, representing the depth to which the ball penetrates the flat sample surface during sliding, and determines the depth of the wear track on the flat sample. The wear behaviour was monitored in accordance to the previously used procedure [17], by measuring the wear scar width and length, after the test and considering the geometry of the contact pair, as well as by using the PD parameter for each test. The wear factor, k, was calculated for each conducted test, according to the following equation:

$$k = V / Fs \quad (1)$$

where F is the normal load, s is the sliding distance, and V is the wear volume. The wear volume of each flat sample was calculated by using the average surface area of the wear track from the image obtained by optical microscopy and the maximum penetration depth (PD) parameter, recorded by the nanotribometer for each test. It was assumed that the cross-sectional area is a flat segment of a sphere, with PD representing the height of that flat segment while further details are shown previously [17]. Since the wear of the stainless-steel ball can be described as "no measurable wear", only the wear of the flat sample was calculated, as per the ASTM G133 standard.

3. RESULTS AND DISCUSSION

SEM images of the wear tracks on PMMA samples, after dry sliding against AISI 316L stainless steel, are shown in Fig. 1. Different magnifications are shown with specific details. *Backscattered* Electron (BSE) image is also shown in Fig. 1 (denoted as BEC).

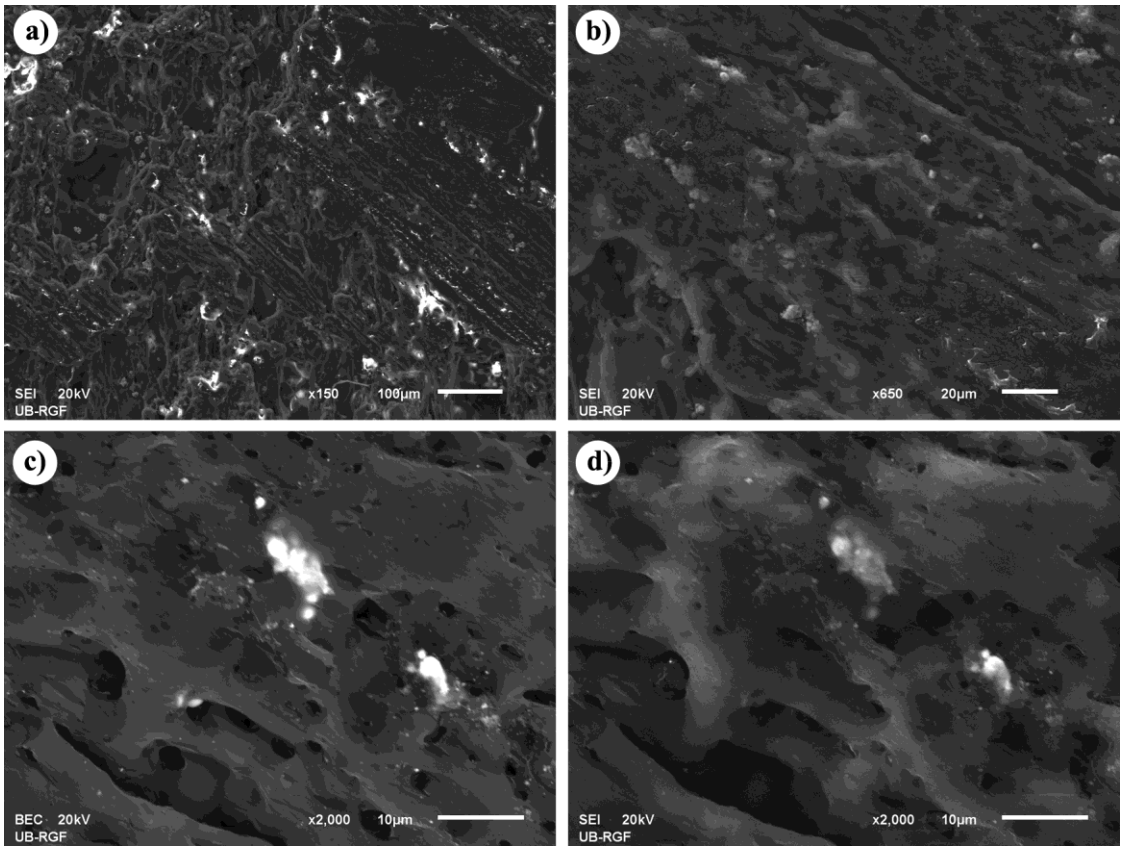

Figure 1. SEM images of the sample surface (dry sliding; 12 mm/s sliding speed; 750 mN normal load): a), b), d) SEM images showing details in the worn track at different magnifications (scale bars: 100, 20 and 10 µm, respectively); c) Backscattered Electron (BSE) image showing difference in chemical compositions in the worn track

The BSE image mode provides elemental contrast, *i.e*. chemical contrast, allowing distinction of the layers with different chemical compositions based on differences in color contrasts. Small white spots in Figure 1c designate ZrO_2 while the grey area represents the PMMA matrix. Secondary electron images obtained by SEM (denoted by *SEI* in Fig. 1) are high-resolution images of shapes of sample surfaces. ZrO_2 particles originate from additives in the PMMA powder component, whereas ZrO_2 is considered as one of the most common radiopaque agents in PMMA [27]. Since these particles are uniformly distributed throughout the PMMA matrix, the PMMA behaviour can be considered as that of a particle reinforced composite. Uniform distribution of these brittle, hard ZrO_2 particles throughout the PMMA matrix has a significant influence on the contact behaviour of the PMMA composite. It can be noticed (Fig. 1) that the wear track is of irregular shape. The evidence of abrasive wear can be clearly observed with many abrasive grooves in the wear track along the direction of sliding. The wear track is discontinued in those areas where pores or cavities occurred on the PMMA surface. ZrO_2 is distributed evenly throughout the whole PMMA surface except in the wear track.

The wear track at the highest investigated sliding speed (Fig. 1a-c) exhibited smooth surface, with shallow scratches and grooves, thus indicating governing adhesive wear. Plastic deformation of the PMMA material during sliding can be also observed in the form of plastic grooving. Areas of plastic deformation are more pronounced within the areas close to the edge of the wear track, along the sliding direction. The central part of the wear track is mainly subjected to abrasive and adhesive wear mechanisms. If the wear track is compared to the rest of the PMMA surface, it can be noticed that ZrO_2 particles are not evenly distributed throughout the wear track as on the rest of the PMMA surface (Fig. 1a). These particles appear smeared on the wear track and less present. A higher magnification (Fig. 1c, d) showed that clusters of ZrO_2 particles (approximately 5 μm in length) were distributed along the direction of sliding. The porous nature of PMMA can be clearly observed in Fig. 1c and d. It appears that PMMA wear tracks undergo plastic deformations – similar to 'work hardening' observed in the strengthening of metals. Increased densification (shrinkage) of PMMA can be observed in the area of the sliding contact (wear tracks) under all contact conditions, while more pronounced under higher sliding speeds and in Ringer's solution, as shown in Figs. 1a, 3a, 5 and 6, and in Supplementary material (Figs. S-1 to S-6).

EDS analyses of the wear tracks on PMMA samples were realised by using the spectrum analysis of selected positions on the sample surface, shown in Figure 2. It was proved that small white spots on the PMMA samples were ZrO_2 (Fig. 2b). Evidence of the abrasive wear, adhesive wear and plastic deformation grooves can be clearly observed in Figure 2a. Larger clusters of ZrO_2 particles were mainly positioned in cavities and pores. Only very small ZrO_2 particles can be observed in areas of pronounced abrasive and adhesive wear. The EDS analysis also proved that there was a transfer of stainless steel to the PMMA surface during sliding, but only in very small amounts, as shown in Figure 2c, approximately up to 0.04 atomic % in the total composition. The EDS analysis was performed at numerous positions and traces of steel transfer were found only at few positions, indicating that the transfer of steel onto PMMA existed at dry sliding, but only to a very small extent. Traces of gold (Au) shown in Figures 2b and c originate from gold deposition on the PMMA surface prior to SEM analysis due to the preparation procedure of PMMA for SEM analysis. Distribution of all elements in spectrums denoted in Fig. 2a is given in in Supplementary material (Table. S-1).

SEM images of cleaned wear tracks on a PMMA sample after sliding in the presence of Ringer's solution is shown in Figure 3 at different magnifications while BSE images indicate zones with different chemical compositions. As in the previous case of dry sliding, ZrO_2 particles can be observed on the PMMA surface. In the case of low sliding speeds, many small ZrO_2 particles were evenly distributed on the PMMA surface, as shown in Supplementary material (Fig. S7). However, in the case of the high sliding speeds (Fig. 3) these particles were present in the smaller extent. Unlike for dry sliding, smearing of ZrO_2 particles clusters along the sliding direction was not noticed (Fig. 3a, b). Clusters of ZrO_2 particles stayed approximately round in shape and larger clusters can hardly be seen in the wear track, while only very small ZrO_2 particles can be observed (Fig. 3c, d). Abrasive grooves can be seen but scratches were not as deep as in the case of dry sliding and adhesive wear was more prominent. Wear tracks are discontinuous, consisting of many small round-shaped areas. This was also observed in the case of dry sliding, but in the case of wet sliding, wear tracks were much more distributed as a number of small round tracks, each exhibiting similar wear mechanisms. In that case, increased densification of PMMA can be observed within the area of the sliding contact (wear tracks) under all contact conditions, also more pronounced under

higher sliding speeds as it was the case of dry sliding. Pores, cavities and PMMA beads clusters can be observed next to edges of the wear tracks (Fig. 3b). Higher magnification (Fig. 3c, d) revealed a similar PMMA structure as in the case of dry sliding, except for the obvious difference in the lack of large clusters of ZrO_2 particles.

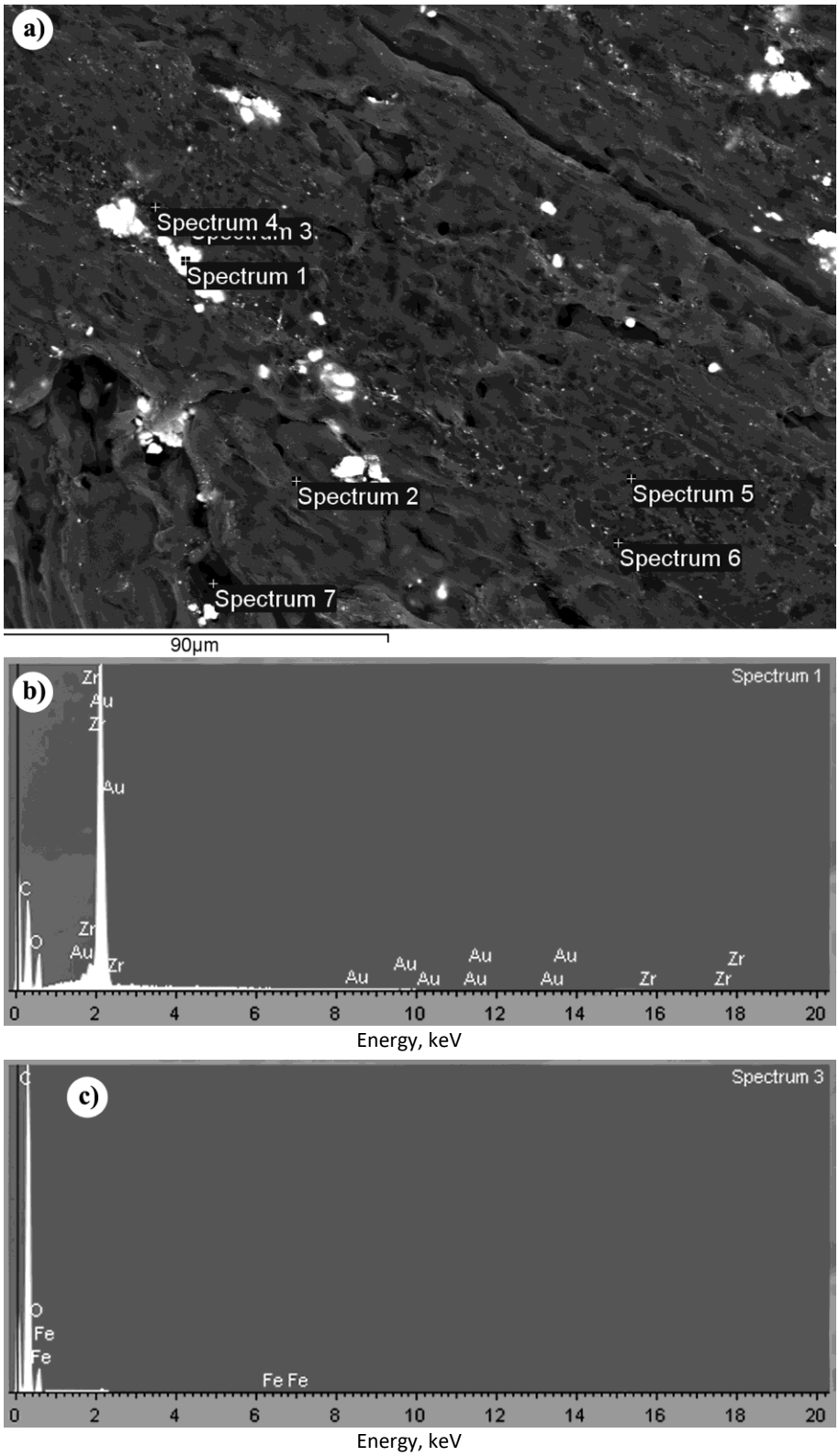

Figure 2. EDS microanalysis of the wear track (dry sliding; 12 mm/s; 500 mN): a) SEM image of the wear track with denoted positions of EDS spectrum analyses; b) EDS analysis (chemical composition) for the position 1; c) EDS analysis for the position 3.

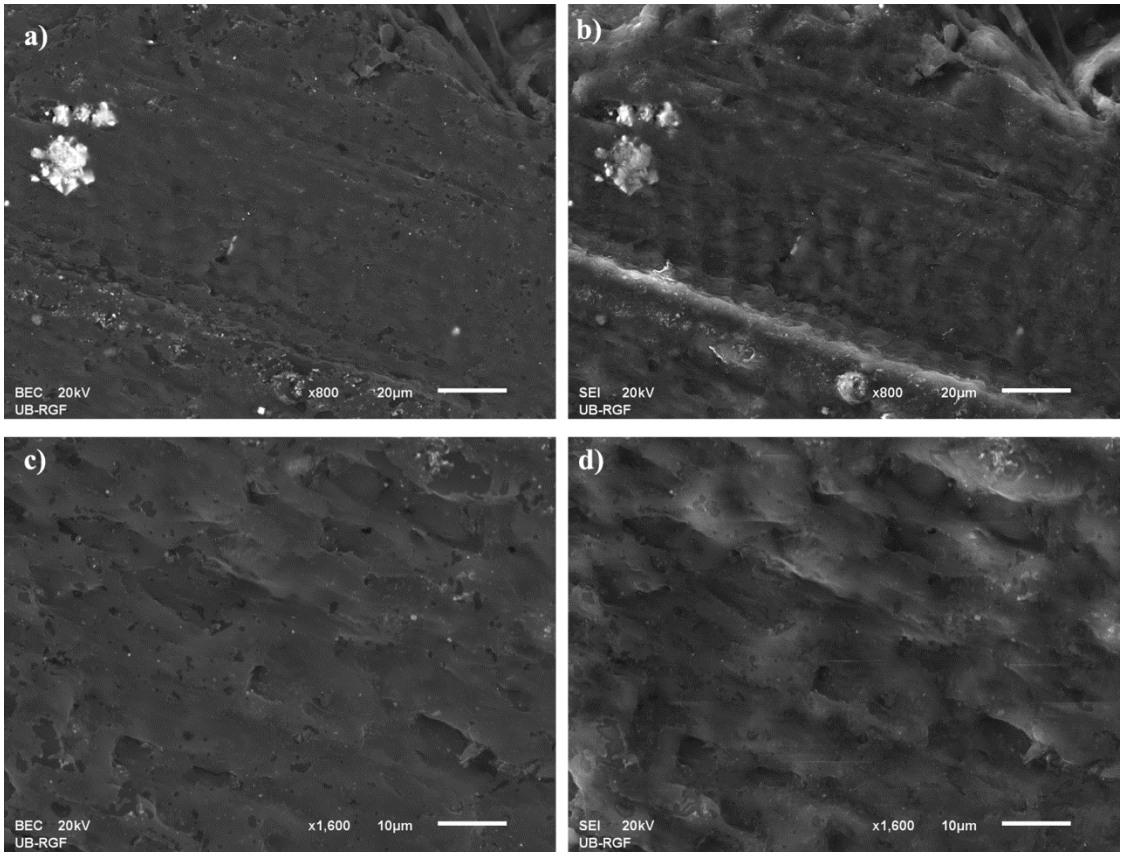

Figure 3. SEM images of the of the wear track (sliding in Ringer's solution; 12 mm/s; 750 mN): a), c) BSE images showing differences in the chemical composition in the wear track; b), d) SEI images of the wear track at different magnifications

EDS analyses of the wear tracks on PMMA samples in the case of wet sliding is shown in Fig. 4. Spectrum positions in Fig. 4 were selected to analyse residuals observed at the surface after sliding. Only elements originating from the PMMA composition and Ringer's solution were detected. The EDS analysis showed traces of Zr (originating from ZrO_2) and Cl (originating from the Ringer's solution) mainly within cavities observed on the surface, just outside of the wear track zones (small round-shaped areas of wear tracks). Small sized ZrO_2 particles can be observed. The EDS analysis in the case of wet sliding showed that the transfer of the steel to the polymer was not occurring unlike for dry sliding. Only residual contents of Na, Cl and K originating from the Ringer's solution were detected. Distribution of all elements in spectrums denoted in Fig. 4a is given in in Supplementary material (Table. S-2).

Several observed phenomena during sliding of PMMA against AISI 316L stainless steel are shown in the following images. A detail in the wear track in the case of dry sliding is shown in Fig. 5. Evidence of fatigue wear, fatigue crack initiation and a crack development pattern are clearly seen. A network of fine random cracks or fissures on the surface of the PMMA wear track (Fig. 5) can be observed, termed craze cracks. These small craze cracks are probably associated with the plastic shrinkage cracking, due to rapid hardening of the surface. They penetrated to a very shallow depth, and further represent the stress initiators.

Fatigue cracks developed normal to the sliding direction (perpendicular to abrasive scratches) growing into large cracks eventually leading to chipping, spalling and detachment of large pieces of densified PMMA surface leaving irregular empty spaces on the surface along the edges of the wear track as clearly observed in Figure 5. Large deep abrasive grooves (Fig. 5) were probably made by detached PMMA particles acting as a third-body abrasive during the contact. Figure 5 shows the evidence of particulate wear debris. In the case of dry sliding, wear tracks were often formed over large voids on the PMMA surface, where these voids originated from the PMMA original structure, which is highly influenced by the initial cement mixing method, surely affecting the sliding contact behaviour. However, development of microcracks within these wear track regions followed the same previously described pattern as well (shown in Fig. 5). Discontinuity of the PMMA matrix material at the position of the void did not change the wear mechanisms: abrasive, adhesive wear, and fatigue. It is

probable that some of the detached PMMA particles are being captured by larger voids and do not further interfere with the sliding process.

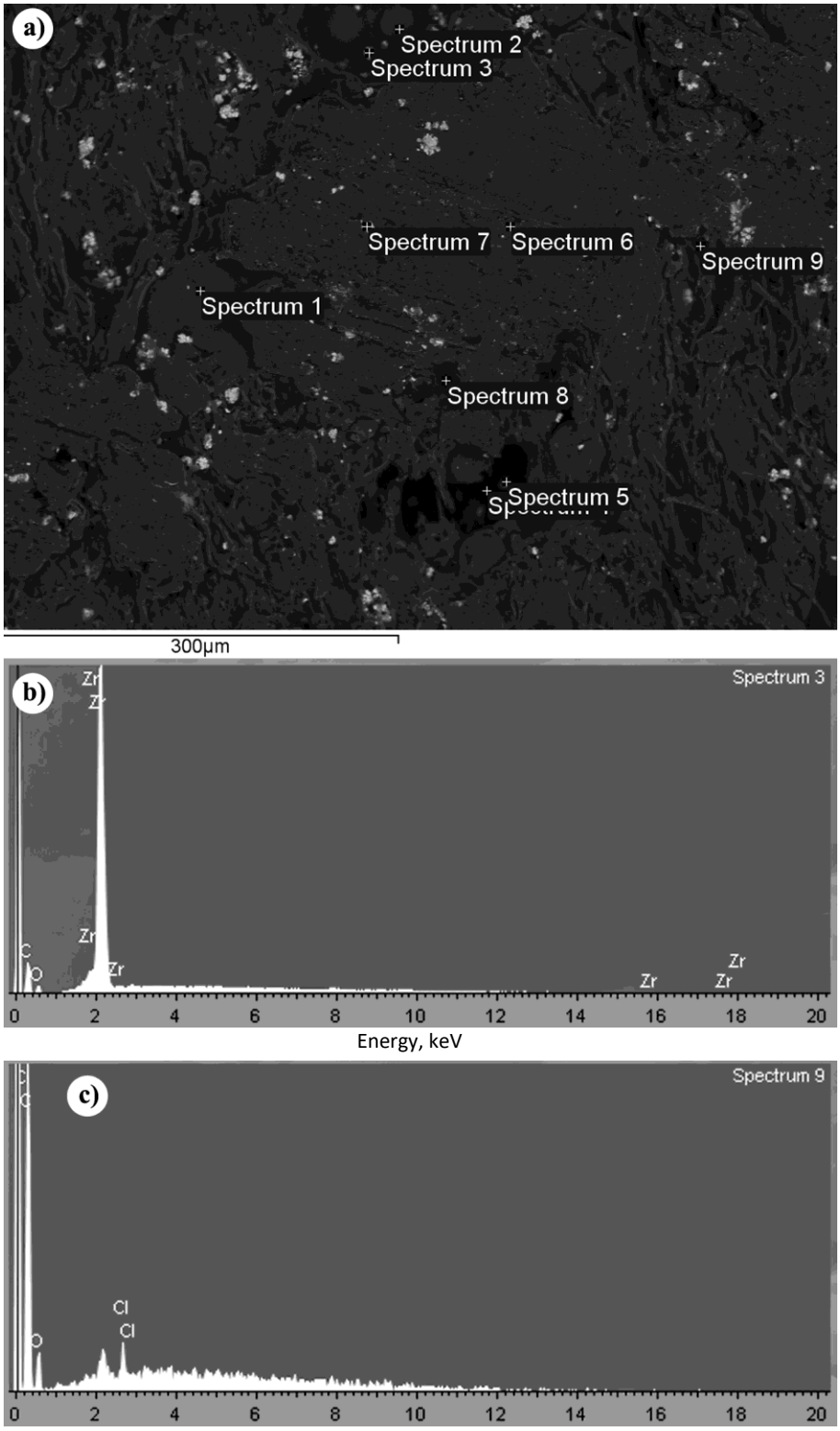

Figure 4. EDS microanalysis of the wear track (sliding in Ringer's solution; 12 mm/s; 750 mN): a) SEM image of the cleaned wear track with denoted positions of EDS spectrum analyses ; b) EDS analysis (chemical composition) for the position 3; c) EDS analysis for the position 9.

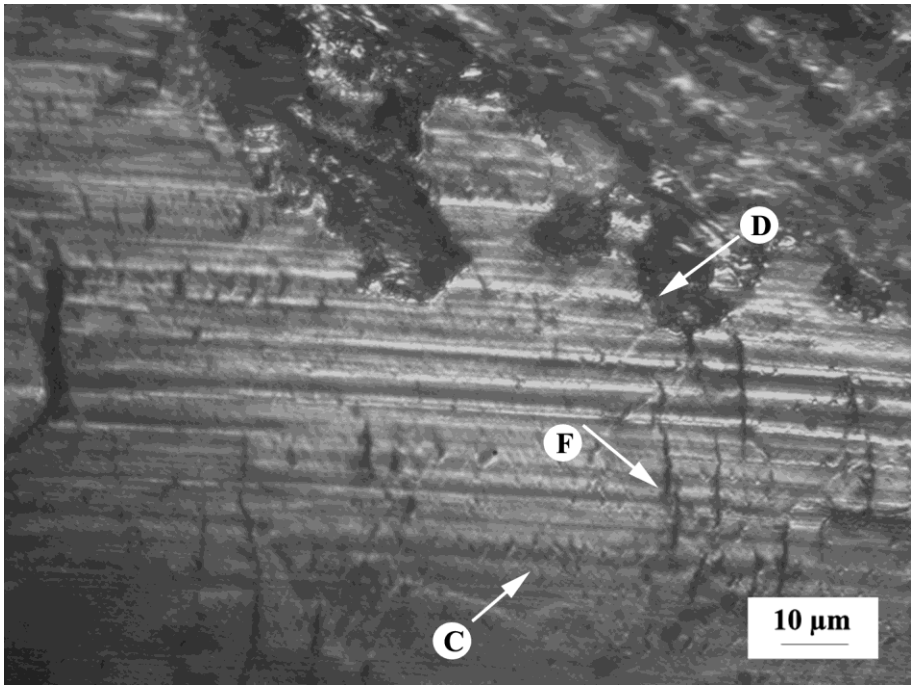

Figure 5. Irregular edges of the wear track, delamination (as denoted by the arrow, D) surface crazing (as denoted by the arrow, C) and fatigue cracks (as denoted by the arrow, F) along the wear track: normal to the sliding direction (dry sliding; 4 mm/s; 500 mN)

It is probable that some of the detached PMMA particles are being captured by larger voids and do not further interfere with the sliding process. However, some part of small PMMA particles affected the wear mechanism producing the three-body wear, clearly evident in Fig. 5 (deep abrasive groove). Detached areas of the PMMA wear track surface shown in Figure 5 in a form of broken edges of irregular shapes have occurred under all test conditions during the dry sliding.

In the case of wet sliding this phenomenon was also observed but with one difference. Detached areas are surrounded with smooth edges as opposed to ragged edges in the previous case and these further developed into regular ellipsoid-shaped cavities as shown in Figure 6b. This was obviously the result of the influence of the Ringer's solution flowing through empty spaces (discontinued material) within the contact zone. These cavities in both cases, dry and wet sliding occurred only on the surface of wear tracks not extending into the bulk material beyond the densified area of the wear track. The cavities were formed by peeling off the surface layers of the wear track on PMMA samples, very similar to spalling of a coating.

In the case of wet sliding, these round cavities were larger in diameters under lower speeds and loads (Fig. 6b) while of significantly smaller sizes under higher speeds and loads. Also, in the case of wet sliding, several small pits can be observed in central regions of the wear tracks, which would probably grow into these large cavities. In the case of dry sliding, such small pits were not observed. These observations are consistent with the published results showing that the increase in the chlorides concentration produced the increase in the number of pits [12]. Fragmentation of wear tracks observed under both sliding conditions was significantly higher in the case of the wet sliding. Large grooves and gouges can be observed throughout the wear tracks under all test wet sliding conditions, as shown in Figure 6, originating from spalled surface layers of the wear track. Fragmentation of the wear track together with the abrasive effect of detached PMMA particles can be clearly observed in Figure 6a.

The wear track appearance shown in Figure 6 is typical for erosion and abrasive wear. Erosion initially is produced by the flow of Ringer's solution within the contact zone. Later when the wear debris starts to form, small PMMA particles mix with Ringer's solution making an erosive slurry, which intensifies the erosion wear by the action of the slurry sliding and flowing on the surface causing additional increases in PMMA particles/layers detachment. The erosive action of the slurry produced significantly wider gouges and grooves under higher speeds and loads, which is consistent with the higher flow of the slurry through these openings at higher sliding speeds. Large erosion grooves and a number of small pits and microcracks developing within the fracture can be observed in Figures 6b and c. A half-detached piece of the

surface layer of the wear track on the PMMA sample can be seen in Figure 6d. It is obvious that the flow of Ringer's solution promoted separation of this half-detached piece of the surface layer.

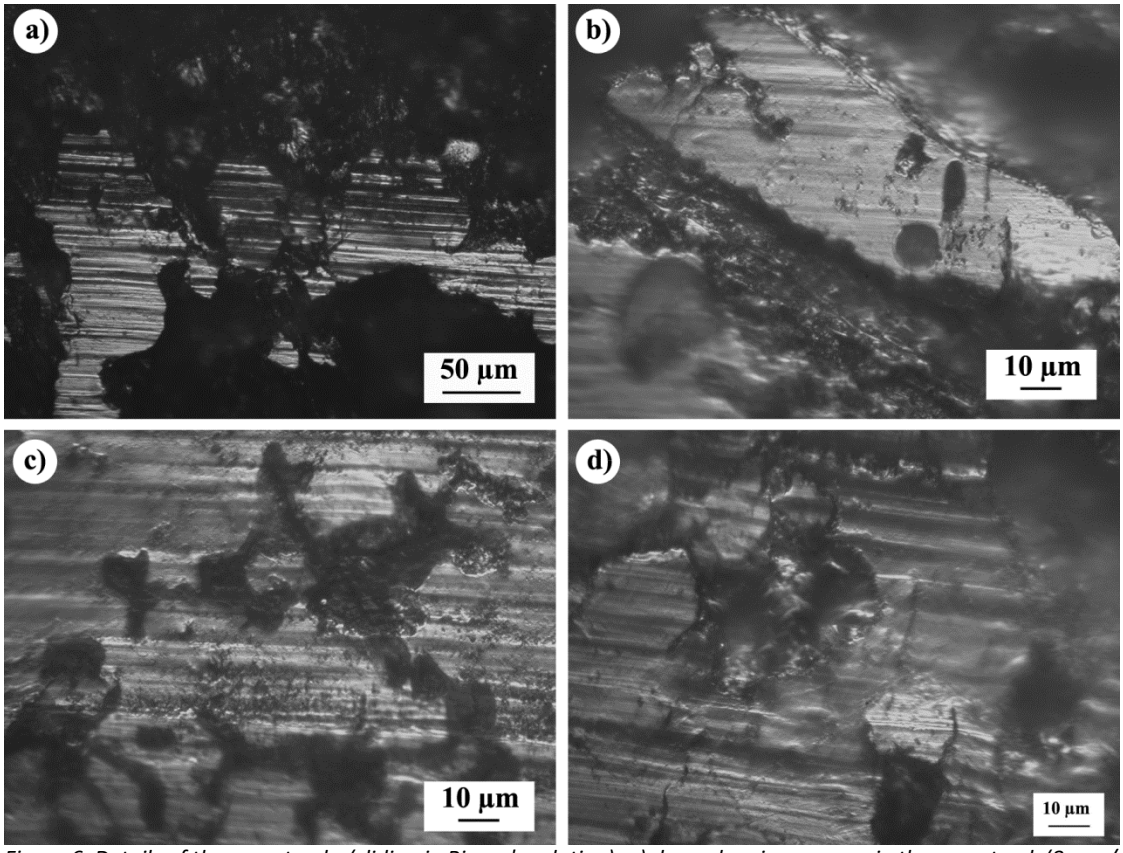

Figure 6. Details of the wear tracks (sliding in Ringer's solution): a) deep abrasive grooves in the wear track (8 mm/s; 250 mN; scale bar: 50 µm); b) details of the wear tracks at 4 mm/s; 100 mN (scale bar: 10 µm); c) deep erosive grooves in the wear track made by the Ringer's solution flow (12 mm/s; 500 mN; scale bar: 10 µm); d) fatigue debris particle in the process of being spalled off the PMMA surface as a result of crack growth at 12 mm/s; 750 mN

Effects of the load and sliding speed on the calculated wear factors in all experiments are shown in Figure 7. The load variations did not induce any significant changes of the wear factor under both test conditions (dry or wet). On the other hand, the increase in the sliding speed induced a significant increase in the wear factor (Fig. 7b, d), more pronounced in the case of dry sliding (Fig. 7b).

Polymers, in general, and PMMA as a visco-elasto-plastic material, are extremely sensitive to frictional heating. It is well known that friction is a typical dissipative process in which mechanical energy is converted into heat (up to 90 - 95 % according to experimental data) [19]. Considering the fact that the increase in the sliding speed is directly associated with the increase in the contact temperature, the wear increase is expected, as it is actually obtained in this study. It should be noted that the increase in the wear factor with the sliding speed increase is significantly higher under dry than under wet conditions (Figs 7 b and d, respectively). The Ringer's solution as a lubricating environment obviously induced lowering of the contact temperature to some extent. On the other hand, wear factors were in average higher for sliding in Ringer's solution than under dry conditions (Fig. 7).

Tiainen [20] studied tribological behaviour of PMMA in contact with different materials (4/10 MPa loads; pin-on-plate reciprocating tests) and reported wear factors of PMMA as: $33/25\times10^{-6}$ mm^3/Nm and $0.086/0.047\times10^{-6}$ mm^3/Nm for CoCrMo and DLC-coated pins, respectively. Recent studies of PMMA wear reported wide ranges of wear rates depending on the PMMA preparation procedure [5,14]. Wear factors of the order of 7×10^{-6} mm^3/Nm can be found in the literature for dry sliding of a steel pin on PMMA, but without details on the steel type or test conditions [5,14]. Wear factors obtained in our study were in the range of $25\text{-}90\times10^{-6}$ mm^3/Nm for dry tests and $90\text{-}130\times10^{-6}$ mm^3/Nm for wet

sliding. Comparison of all produced wear tracks within our study, for the same test regimes for dry and wet sliding, evidently indicated that in the former case the wear tracks were irregularly shaped with uneven edges. On the opposite, wet sliding produced more regularly shaped, often rounded wear tracks. Under reciprocating sliding, the investigated bone cement displayed a true mechanical fatigue failure in both environments. In the case of wet sliding, lower loads produced deep abrasive grooves along the sliding direction, while higher loads produced lower number of scratches not as deep as in the case of dry sliding and sliding under lower loads.

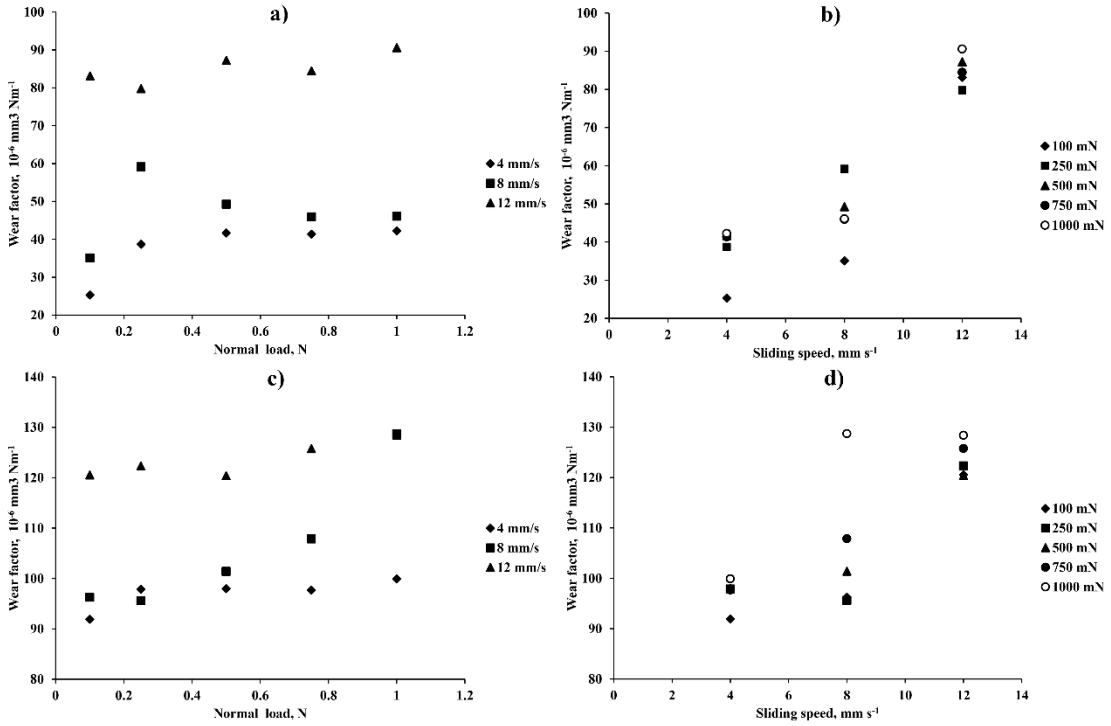

Figure 7. Wear factor of PMMA samples as a function of the normal load at different sliding speeds under: a) dry sliding, c) sliding in Ringer's solution; as a function of the sliding speed at different normal loads under: b) dry sliding, d) sliding in Ringer's solution

Several authors investigated the fracture properties (constant amplitude fatigue, fatigue crack propagation and plane-strain fracture toughness) of bone cements [2] or the fatigue failure process and the earliest stages of crack initiation in an acrylic bone cement [9,10]. It was reported that in the presence of a pore, crack initiation may occur away from the pore due to the combined influence of pore morphology and the presence of defects within regions of stress concentration. Small cracks associated with porosity have not been seen in the control specimens, whereas a fatigue crack initiation site occurred in the vicinity of a pore [9]. In a study of the impact and compression damage of PMMA spheres over a range of loads and velocities it was found that radial crazing always formed under compressive loads indicating large amounts of energy dissipation by inelastic deformations [21]. This is in consistence with observed cracks in Figure 5 where surface crazing and fatigue cracks are evident.

Several studies investigated the non-steady crack and craze behaviour of PMMA under cyclical loading [16,22]. The traditional engineering approach to fatigue description in metals and in the presence of a crack is to relate the stress intensity factor to the average crack propagation rate (per cycle). With respect to polymers there exist two features that set these materials apart. One is the fact that because of their intrinsic time or rate sensitive characteristics the growth of a crack does not depend greatly on the number of cycles but (also) on the frequency as a parameter representing the time history [22]. Furthermore, it seems that the crack does not propagate steadily but in 'spurts' and that these spurts depend on the load level and time history. Under the test conditions conducted in our study, increases in the load and sliding speed produced significantly more cracks, even though the increase in the first parameter did not produce the wear factor increase.

At low crack-growth rates (as in the case of dry sliding in our study), the crack is able to find the easiest path through the microstructure, perhaps around the PMMA beads themselves. Thus, the crack follows a torturous path, and the fracture surfaces are highly irregular and uneven. Here, the evidence of particulate wear debris was the most apparent. At higher fatigue crack-growth rates (as in the case of wet sliding here), the fracture surfaces are progressively less rough as the crack apparently becomes less sensitive to local microstructural features (Fig. 6b). In addition, the fracture surfaces exhibited significantly smaller amounts of the wear debris and began to show signs of PMMA bead cleavage (Fig. 3b). It was proved that physiological environment has a profound effect upon both the cyclic fatigue crack-growth and fracture toughness behaviour of PMMA bone cements [10, 16]. PMMA was found to be more resistant to both cyclic fatigue and fracture in Ringer's solution than in laboratory air with 45% relative humidity, which is due to both the lubricating effect of the aqueous environment and its effect on increasing ductility in the polymer [10]. During the toughness testing in Ringer's solution [10], in the case of fast fracture surfaces, the crack cleaved cleanly through all the PMMA beads in the bone cement, leaving behind a smooth, almost flat fracture surface. In contrast, during the testing in air, fracture surfaces were relatively rough, and some PMMA beads remain uncleaved [10]. This agrees with our results. Cleaved PMMA beads can be clearly observed in Figure 3b, while uncleaved PMMA beads can be observed in Figure 2a.

For both dry and wet sliding, comparison of appropriate wear tracks for the same load regimes indicated that the higher loads produced more uniform and less fragmented wear tracks, probably meaning that higher loads induced higher densification of the PMMA bone cement surface. But the wear factor did not significantly change with load changes, oscillating around a mean value, in both cases of dry and wet sliding. It seems that the load change is compensated by the induced plastic deformations in PMMA. Some authors proved that the maximal densification occurs at the temperature equal to the pressure induced glass transition temperature, Tg (around 105 ^{o}C for PMMA), and that PMMA densification starts well below Tg at zero pressure [23]. Temperature affects physical properties of polymers and hence storage modulus (elastic portion) of PMMA is almost two times lower at 80 ºC than at the room temperature [23].

Friction heating generated during the sliding contact, enhanced plastic deformation of the PMMA bone cement and its densification, which is achieved by the mass transport into the pores thus producing a decrease in the pore volume. However, different pressure holding times do not influence density profiles of PMMA and densification is not proportional to the pressure applied [2]. This is consistent with of the obtained results that the wear factor did not depend on the load change (Fig. 7a, c).

Due to multiple ions in Ringer solution (Na^+, K^+, Ca^{2+}, Cl^-), attraction and friction phenomena are difficult to identify. It can be expected that chlorides from the Ringer's solution produce metal dissolution. It was shown that chlorides induce disruption of passive films and promote dissolution of the metal due to the driving force by formation of metallic complexes on the 316L surface (*e.g.* α-Cr_2O_3, Fe_3O_4) [24]. However, the EDS analysis in our wet tests (Fig. 4) showed that steel was not transferred to the polymer. It was shown in literature that PMMA surface charges are negative while 316L surface charges are positive [24], so that the dissolution of metal ions reinforces attraction between the surfaces. On the other hand, high roughness of bone cement samples promotes disruption of the oxides film. Also, due to the high roughness, separation between the contact surfaces is too large to consider the contribution of electrostatic forces. According to literature [24], when the roughness is higher than 1 nm for bone cement samples, attraction does not occur between surfaces, indicating that the electrostatic forces can be neglected in the case of 316L - cement contact in our study.

However, Ringer's solution increased the wear factor if compared to dry sliding. It is probable that multiple ions in Ringer's solution influenced the 316L corrosion wear, producing corrosion debris thus adding to the third body wear (increasing PMMA worn particles) and promoting higher adhesion wear, and altogether increasing the wear level. Also, it was proved that the corrosion damage of steel increases when it is stressed, especially under compressive stresses [25]. The presence of the Ringer's solution in the contact zone prevented formation of large clusters of bone cement wear debris, otherwise promoted under dry conditions. Large PMMA clusters promote third-body abrasion and formed deep abrasive grooves (such as in Fig. 5), but they are also prone to easier ejection out of the contact zone. The PMMA wear debris in Ringer's solution consisted of small size particles, thus promoting polishing of the PMMA surface, which

can be clearly seen by comparison of Figures 1 and 3. On the other hand, flow of the erosive slurry formed by Ringer's solution and PMMA wear debris promotes early detachment of half broken pieces of surface layers in the wear track (Fig. 6d) thus increasing the wear level and producing large gouges and grooves (Fig. 6).

Several studies indicate that micromechanisms of fracture in PMMA promote formation of an energy dissipation zone surrounding the crack [16]. This zone arises primarily from crazing ahead of the crack tip but may lead to crack bridging on the subsequent crack extension by uncracked matrix ligaments and shielding of the crack tip by the dilated crazed zone in the wake of the crack [10]. These processes depend on the crack length and can have a profound effect on the toughness of the material. Whitening (crazing) of the bone cement around newly formed crack is evident in Figure 3. The stress whitening is a consequence of the craze cracks that appear prior to the crack propagation [16]. It was reported that a bone cement was considerably more resistant to fatigue-crack propagation in Ringer's solution than in air [10]. The increased PMMA toughness in Ringer's solution is thought to arise from the plasticizing effect of the environment [10,18]. A similar effect of has been also reported for other brittle materials, while such effect is not consistent with the fatigue crack-growth behaviour in metallic materials where toughness is relatively insensitive to crack growth rates [10]. On the other hand, the plasticizing effect enhances crazing in the crack tip region and leads to an increased fracture toughness. The presence of soluble environmental agents is well known to reduce the critical stress or strain required to initiate crazing [10]. Decreased stresses influenced by Ringer's solution result in a significantly larger craze or plastic zone size ahead of the crack tip as shown in Figures 3b and d.

Water has been known to have a plasticizing effect on polymers [16,18,26]. Water molecules act to break intermolecular bonds of the polymer, thus increasing the chain mobility and reducing the strength. Immersion in water is comparable to the effect of a rise in temperature according to literature [18]. This is consistent with results of our study where Ringer's solution increased the wear factor when compared to that under dry sliding, similarly as the increase of this parameter due to the increase in the sliding speed (due to the increase in the contact temperature). In a previous study it was shown that the influences of Ringer's solution and distilled water on curing or creep properties of PMMA bone cement were not significantly different [18], indicating that physiological salts present in Ringer's solution do not induce additional effects on curing or creep deformation. It is known that in glassy polymers (*e.g*. PMMA), water tends to move to free volume regions created by local defects [16]. This is also found in our study by the EDS analysis showing residual contents of Cl, Na and K from Ringer's solution only in voids and cavities observed on the sample surface (Fig. 4). On the other hand, these regions strongly contribute to deformation and fatigue crack initiation, as elaborated in literature [15]. The increase in the sliding speed had more drastic effects in the case of dry sliding, while under wet sliding conditions the increase in the wear factor was rather moderate. At sliding speeds and thus higher temperatures, the chain mobility of the PMMA has already increased to such an extent that additional water plasticization had little effects. This is the main difference of dry and wet sliding in relation to the wear factor dependences shown in Figures 7b and d: the wear factor has already been shifted to higher values at lower speeds and further increase is moderate under wet conditions, unlike for dry sliding where the wear factor increase is steeper.

PMMA wear debris has been studied in literature [27] showing that poorly mixed PMMA may release pre-polymerized spheres 25 - 35 μm in size. Small movements between the implant and the PMMA mantle or the PMMA implant and bone may constantly produce PMMA particles. For example, it was reported that micron and sub-micron particles or smaller particles of cement radiopaque agents such as ZrO_2 are contained in PMMA voids [27]. This is consistent with results obtained in our study (Figs. 1-4). Accumulation of ZrO_2 particles 10 - 15 μm in size, is clearly seen in Figure 3a while micron and sub-micron sized ZrO_2 particles or particle aggregates can be clearly observed in Figures 1c and d. In addition, pre-polymerized PMMA spheres in the size range 25 - 35 μm can be clearly seen in Figure 3b. According to literature [27] PMMA particles or associated voids can be described as: fine particles (<1 μm in size), multifaceted fragments with sharp edges (1 - 5 μm in size; more common than previous ones), spherical particles (5 - 25 μm in size), and even beads with pits and cracks (20 - 200 μm in size) or irregular chunks about 1 mm in length. One PMMA particle approximately 15 μm in size can be seen in Figure 6d, as a beginning of the wear debris formation by delamination. Hard debris such as PMMA particles and especially hard ZrO_2 particles induce scratching and produce plowing grooves, clearly visible in wear tracks (Figs. 5 and 6a). The effects of radiopaque agents (*e.g*. zirconium oxide

(ZrO_2)) on cement behaviour have been investigated in literature [8], especially regarding static mechanical properties, such as fatigue, while some studies considered also the physiological effects. Radiopaque agent particles (usually hard ceramic particles) could leach out of the material and find their way to the joints and become trapped in the joint component (if made of polymers), scratching the metallic component. They could also cause osteolysis if they penetrate the interface with the bone cavity. These particles in the cement produce worsening of the mechanical properties as a consequence of the stress concentration around the particles [8]. Some studies aimed to improve dispersion of the inorganic particles in order to improve the cement fatigue properties. The question of whether to perform the mixing in vacuum or manually in open atmosphere has been addressed by several researchers [1]. Ultimately, mixing in vacuum is widely recommended over the hand-mixing technique in order to obtain cements that will retain appropriate levels of hardness and elasticity for at least 2 or 3 decades whilst implanted *in vivo*, even though the optimal vacuum regime and optimal cement porosity are still under debate. Results obtained in our earlier study indicated that a combination of different periods of vacuum treatment of the bone cement produced good results regarding mechanical properties [6]. This in return, should induce less wear debris during sliding.

4. CONCLUSION

This research has aimed at the influence of the Ringer's solution on the wear of vacuum mixed PMMA bone cement during the reciprocating sliding with AISI 316L stainless steel, at low loads, in order to simulate the contacts that frequently appear in medical implants. Sliding in Ringer's solution was compared to dry sliding and crack initiation and development was analysed. Dry sliding produced discontinued, irregularly shaped wear tracks with a clear evidence of strong abrasive, adhesive wear, and plastic deformation grooves. The increase in the sliding speed produced smoother wear tracks with more pronounced adhesive wear. Plastic deformation along the sliding direction is more evident closer to the edges of the wear track. Also, under these conditions, aggregation and smearing of ZrO_2 particles occurred throughout the wear track. Larger clusters of ZrO_2 particles were mainly positioned in cavities and pores. Also, there was a slight transfer of stainless steel to the PMMA surface during sliding. Prominent fatigue wear and fatigue crack initiation were observed, as well as networks of fine random cracks on the cement surface. Fatigue cracks developed in the direction normal to sliding (perpendicular to abrasive scratches) growing into the large cracks and leading to chipping, spalling and detachment of large pieces of densified PMMA surface and producing three-body wear. The wear debris particles varied in size, from small fine particles, below 1 μm up to 15 μm and larger, according to associated voids formed on the polymer surface.

In the case of sliding in the presence of Ringer's solution, abrasive grooves could be seen but scratches were not as deep as in the case of dry sliding and adhesive wear was more prominent. Steel was not transferred to the polymer surface. Wear tracks were also discontinuous, consisting of many small mainly round-shaped areas. Aggregation of ZrO_2 particles was also exhibited but to a significantly smaller extent and the particles were mainly rounded without smearing along the sliding direction. Detached parts of the cement surface formed smooth edges further developing into rather regular ellipsoid-shaped cavities, showing the influence of the Ringer's solution flow within the contact zone. Erosion and abrasive wear were prominent, but fatigue failure was also present. Large erosion grooves, number of small pits and microcracks developing into fractures could be observed.

In both cases of dry and wet sliding, cavities and voids formed only on the surface of the wear track and did not extended into the bulk material beyond densified area of the wear track. Fragmentation of wear tracks observed in both cases was significantly higher in the case of wet sliding.

Changes in the load over the investigated range did not produce any significant effect on wear factor values for both test conditions. Higher loads produced more uniform and less fragmented wear tracks, probably meaning that higher loads induced higher densification of the PMMA bone cement surface. The increase in the sliding speed induced significant increases in the wear factor, more pronounced in the case of dry sliding. Wear factors were in average higher for sliding in Ringer's solution than under dry conditions.

These findings provide significant insights into the patterns of surface cracks in PMMA bone cements, during its contact with a steel implant in physiological environments. Results indicated that craze cracks have important role in

damage behaviour of PMMA cements, beside fatigue cracks that altogether determine the life of the implant subjected to a complex micromotions.

Acknowledgements: The research study was financed by the Ministry of Education, Science and Technological Development, Serbia, project No. 451-03-68/2020-14/200107, and project No. 451-03-68/2020-14/200105.

REFERENCES

[1] Boote AT, Bigsby RJ, Deehan DJ, Rankin KS, Swailes DC, Hyde PJ. Does vacuum mixing affect diameter shrinkage of a PMMA cement mantle during in vitro cemented acetabulum implantation? *Proc Inst Mech Eng, Part H.*2021; 235: 133–140.

[2] Lewis G. Viscoelastic properties of injectable bone cements for orthopaedic applications: State-of-the-art review. *J Biomed Mater Res, Part B*. 2011; 98B(1): 171-191.

[3] Stojkovic M, Milovanovic J, Vitkovic N, Trajanovic M, Grujovic N, Milivojevic V, Milisavljevic S, Mrvic S. Reverse modeling and solid free-form fabrication of sternum implant. *Australas Phys Eng Sci Med*. 2010; 33(3): 243-250.

[4] Garcés GA, Rojas VH, Bravo C, Sampaio CS. Shear bond strength evaluation of metallic brackets bonded to a CAD/CAM PMMA material compared to traditional prosthetic temporary materials: an in vitro study. *Dental Press J Orthod*. 2020; 25(3): 31-38.

[5] Reyes-Sevilla M, Kuijs RH, Werner A, Kleverlaan CJ, Lobbezoo F. Comparison of wear between occlusal splint materials and resin composite materials. *J Oral Rehabil*. 2018; 45(7): 539-544.

[6] Zivic F, Babic M, Grujovic N, Mitrovic S, Favaro G, Caunii M. Effect of vacuum-treatment on deformation properties of PMMA bone cement. *J Mech Behav Biomed Mater*. 2012; 5(1): 129-138.

[7] Kraaij G, Zadpoor AA, Tuijthof GJM, Dankelman J, Nelissen RGHH, Valstar ER. Mechanical properties of human bone–implant interface tissue in aseptically loose hip implants. *J Mech Behav Biomed Mater*. 2014; 38: 59-68.

[8] Wimhurst JA, Brooks RA, Rushton N. The effects of particulate bone cements at the bone-implant interface. *J Bone Jt Surg*. 2001; 83-B(4): 588-592.

[9] Sinnett-Jones PE, Browne M, Moffat AJ, Jeffers JRT, Saffari N, Buffière J-Y, Sinclair I. Crack initiation processes in acrylic bone cement. *J Biomed Mater Res A*. 2009; 89A(4): 1088-1097.

[10] Nguyen NC, Maloney WJ, Dauskardt RH. Reliability of PMMA bone cement fixation: fracture and fatigue crack-growth behaviour. *J Mater Sci Mater Med*. 1997; 8(8): 473-483.

[11] Shih C-C, Shih C-M, Su Y-Y, Lin S-J. Potential risk of sternal wires. *Eur J Cardiothorac Surg*. 2004; 25(5): 812-818.

[12] Geringer J, Pellier J, Cleymand F, Forest B. Atomic force microscopy investigations on pits and debris related to fretting-corrosion between 316L SS and PMMA. *Wear*. 2012; 292-293: 207-217.

[13] Koistinen AP, Korhonen H, Kröger H, Lappalainen R. Interfacial sliding properties of bone screw materials and their effect on screw fixation strength. *J Appl Biomater Func*. 2014; 12(2): 90-96.

[14] Takamizawa T, Barkmeier W, Tsujimoto A, Scheidel D, Erickson R, Latta M, Miyazaki M. Mechanical Properties and Simulated Wear of Provisional Resin Materials. *Oper*. 2015; 40(6): 603-613.

[15] Alexeev AA, Bolshev KN, Ivanov VA, Syromyatnikova AS, Bolshakov AM, Andreev AS. Experimental Study of Crack Branching Velocity in Polymers. *Inorg Mater*. 2019; 55(15): 1476-1480.

[16] Koch S, Meunier M, Hopmann C, Alperstein D. A combined experimental and computational study of environmental stress cracking of amorphous polymers. *Polym Adv Technol*. 2020; 31(2): 297-308.

[17] Zivic F, Babic M, Mitrovic S, Vencl A. Continuous control as alternative route for wear monitoring by measuring penetration depth during linear reciprocating sliding of Ti6Al4V alloy. *J Alloys Compd*. 2011; 509(19): 5748-5754.

[18] Arnold JC, Venditti NP. Effects of environment on the creep properties of a poly(ethylmethacrylate) based bone cement. *J Mater Sci: Mater Med*. 2001; 12(8): 707-717.

[19] Myshkin NK, Pesetskii SS, Grigoriev AY. Polymer Tribology: Current State and Applications. *Tribol Ind.* 2015; 37(3): 284-290.

[20] Tiainen V. Amorphous carbon as a bio-mechanical coating — mechanical properties and biological applications. *Diamond Relat Mater*. 2001; 10(2): 153-160.

[21] Gorham DA, Salman AD, Pitt MJ. Static and dynamic failure of PMMA spheres. *Powder Technol*. 2003; 138(2-3): 229-238.

[22] Pulos GC, Knauss WG. Nonsteady crack and craze behavior in PMMA under cyclical loading: I. Experimental preliminaries. *Int J Fract*. 1998; 93(1/4): 145-159.

[23] Etienne S, Becker C, Ruch D, Grignard B, Cartigny G, Detrembleur C, Calberg C, Jerome R. Effects of incorporation of modified silica nanoparticles on the mechanical and thermal properties of PMMA. *J Therm Anal Calorim*. 2007; 87(1): 101-104.

[24] Geringer J, Atmani F, Forest B. Friction–corrosion of AISI 316L/bone cement and AISI 316L/PMMA contacts: Ionic strength effect on tribological behaviour. *Wear*. 2009; 267(5-8): 763-769.

[25] Munir S, Walsh WR. The Quantification of Corrosion Damage for Pre-stressed Conditions: A Model Using Stainless Steel. *Journal of Bio- and Tribo-Corrosion*. 2016; 2(1): 4.

[26] Ayre WN, Denyer SP, Evans SL. Ageing and moisture uptake in polymethyl methacrylate (PMMA) bone cements. *J Mech Behav Biomed Mater*. 2014; 32: 76-88.

[27] Savio JA, Overcamp LM, Black J. Size and shape of biomaterial wear debris. *Clin Mater*. 1994; 15(2): 101-147.

[28] Capitanu L, Badita L-L, Florescu V. Stability Loss of the Cemented Stem of Hip Prosthesis due to Fretting Corrosion Fatigue. *Tribol Ind* 2017; 39(4): 536-546.
[29] De Baets T, Waelput W, Bellemans J. Analysis of third body particles generated during total knee arthroplasty: Is metal debris an issue? *The Knee*. 2008; 15(2): 95-97.

SAŽETAK

Uticaj Ringerovog rastvora na habanje vakuumski tretiranog koštanog cementa od poli(metil metakrilata) u kontaktu sa AISI 316L nerđajućim čelikom pri linearno naizmeničnom kretanju

Fatima Živić[1], Nenad Grujović[1], Slobodan Mitrović[1], Jovan Tanasković[2] i Petar Todorović[1]

[1]*Univerzitet u Kragujevcu, Fakultet inženjerskih nauka, Kragujevac, Srbija*
[2]*Univerzitet u Beogradu, Mašinski fakultet, Beograd, Srbija*

(Naučni rad)

U radu su prikazane mikrostrukturne karakteristike i ponašanje PMMA koštanog cementa mešanog u vakuumu, pri kontaktu sa AISI 316L nerđajućim čelikom, sa mikro opterećenjima i analiziran je uticaj prisustva Ringerovog rastvora na habanje u odnosu na suvi kontakt. Promena sile nije značajno uticala na faktor habanja dok je povećanje brzine klizanja uslovilo značajan porast faktora habanja, naročito u slučaju suvog kontakta. Faktori habanja su u proseku bili veći za klizanje u Ringerovom rastvoru od suvog kontakta. Uočena je značajna fragmentacija tragova habanja, nepravilnog oblika, sa izlomljenim ivicama, što je bilo više naglašeno pri suvom kontaktu. U tragovima habanja se uočavaju brojni otvori i šupljine, koji se ne šire u dubinu materijala. Veća opterećenja su uzrokovala uniformnije i manje fragmentirane tragove habanja. Uočeno je abrazivno i adhezivno habanje i tragovi plastične deformacije, kao i zamorno i erozivno habanje. Zamorne pukotine su se širile u pravcu normalnom na pravac klizanja. Fina mreža tankih površinskih lomnih pukotina je uočena na površini tragova habanja, posebno u slučaju suvog kontakta. Rezultati su značajni kao doprinos razumevanju inicijacije pukotina i mehanizmima njihovog razvoja na površini PMMA koštanog cementa, uključujući i sinergijske efekte fiziološke okoline s aspekta nestacionarnog ponašanja i modela razvoja pukotina kod PMMA.

Ključne reči: lomne pukotine; erozivni useci; lom; denzifikacija; frikciona toplota; zamorni lom.